Optics and Laser Technology 130 (2020) 106331

Contents lists available at ScienceDirect

Optics and Laser Technology

journal homepage: www.elsevier.com/locate/optlastec

Full length article

Customised structural, optical and antibacterial characteristics of cinnamon nanoclusters produced inside organic solvent using 532 nm Q-switched Nd:YAG-pulse laser ablation

Ali Aqeel Salim[a,*], Hazri Bakhtiar[a], Sib Krishna Ghoshal[a,*], Fahrul Huyop[b]

[a] Laser Center and Physics Department, Faculty of Science, UniversitiTeknologi Malaysia, 81310 Johor Bahru, Johor, Malaysia
[b] Biosciences Department, Faculty of Science, UniversitiTeknologi Malaysia, 81310 Johor Bahru, Johor, Malaysia

HIGHLIGHTS

- Spherical Cin-NCs were prepared in citric acid via nanosecond pulse laser ablation.
- Physiochemical traits of these NCs strongly depended on the laser fluence.
- Morphology and structure of Cin-NCs was controlled via laser fluence variation.
- Cin-NCs containing cinnamaldehyde compounds showed strong antibacterial action.
- Achieved Cin-NCs were shown to be favorable for antibacterial drug development.

ARTICLE INFO

Keywords:
PLAL
Cin-NCs
Citric acid medium
Absorption
Antibacterial action

ABSTRACT

Biomedical values of organic natural cinnamon that are buried in their bulk counterpart can be exposed and customised via nanosizing. Based on this factor, a new type of spherical cinnamon nanoclusters (Cin-NCs) were synthesised using eco-friendly nanosecond pulse laser ablation in liquid (PLAL) approach. As-grown nontoxic Cin-NCs suspended in the citric acid of pH 4.5 (acted as organic solvent) were characterised thoroughly to evaluate their structural, optical and bactericidal properties. The effects of various laser fluences (LF) at the fixed wavelength (532 nm) on the physiochemical properties of these Cin-NCs were determined. The FTIR spectra of the Cin-NCs displayed the symmetric-asymmetric stretching of the functional groups attached to the heterocyclic/cinnamaldehyde compounds. The HR-TEM image of the optimum sample revealed the nucleation of the crystalline spherical Cin-NCs with a mean diameter of approximately 10 ± 0.3 nm and lattice fringe spacing around 0.14 nm. In addition, the inhibition zone diameter (IZD) and optical density (OD_{600}) of the proposed Cin-NCs were measured to assess their antibacterial potency against the *Staphylococcus aureus* (IZD ≈ 24 mm) and *Escherichia coli* (IZD ≈ 25 mm) bacterial strains. The strong UV absorption (in the range of 269 and 310 nm) shown by these NCs was established to be useful for the antibacterial drug development and food treatment.

1. Introduction

Resolving the human risks against the pathogenic bacteria or viral diseases remain an ever-ending challenge in the pharmaceutical and biomedicine drug development industries [1]. Indeed, numerous bacterial infections are the reason for varieties of dangerous diseases worldwide, where millions of cases and annual deaths have been reported [2,3]. The *Escherichia coli* (E. coli) and *Staphylococcus aureus* (S. aureus) are the well-known harmful bacteria strains responsible for several untreated diseases (for example food poisoning, diarrhea, cholera, skin irritation, tuberculosis, diphtheria and typhoid) [3,4]. Recently, constant efforts have been made to boost the safety, productivity and affordability in the prevention of such bacteria through the use of various natural herbs integrated in the nanoparticles (NPs) [5,6].

For ages, the natural cinnamon bark/extract (Cin) is popular as the spice, medication assisted treatment and bioactive agent due to the existence of polyphenolic, flavonoids, cinnamaldehyde, coumarin, cinnamic acid and heterocyclic compounds that contains low molecular weight polyphenol [6,7]. Such active cinnamomic elements and their

* Corresponding authors.
E-mail addresses: asali@utm.my (A.A. Salim), sibkrishna@utm.my (S.K. Ghoshal).

https://doi.org/10.1016/j.optlastec.2020.106331
Received 10 January 2020; Received in revised form 26 March 2020; Accepted 8 May 2020
Available online 21 May 2020
0030-3992/

condimental properties have unpredictably varying pharmacological functions including anti-cancer, anti-bacterial, anti-viral and anti-ageing [5–8]. On top, various phytochemical studies on the cinnamon bark (cassia) have been long-established in *vitro* and *vivo,* revealing the existence of diterpenes, sesquiterpenoids, phenylpropanoids and flavonoids without any side effect or toxicity [8]. Despite these promising curative features, the extensive utilization of the cinnamon bark as an active biocidal agent is very minimal and low in pharmacodynamics action due to its poor dispersal and aqueous solubility as well as the lower absorption in the gastrointestinal process, and rapid metabolism to decrease foodstuffs (coumarin, di-tetra, hexahydrocinnamon, heterocyclic, eugenol, flavonoids and cinnamaldehyde) [6–9].

Of late, the organic nanoclusters (ONCs) emerged as an active agent in the area of advanced drug delivery, nanomedicinal, hyperthermia therapy and anti-bacterial purpose [9,10]. The conventional ONCs from their bulk sources can be obtained using the nanotechnology route. These tiny ONCs reveal enhanced pharmacological effects with improved solubilisation, biocompatibility, pharmacokinetic profile and the drug formulation [10]. In the nanoscale structures (nanoparticles or NCs, nanorods, nanowires, nanotubes, nanofilms, nanofluid, etc.), the surface area to volume is significantly large, leading to the emergent physiochemical traits (such as efficient reactivity) that are absent in their bulk counterparts. More interesting features of these ONCs are related to the excellent interfaces with organic/genetic macromolecules such as membranes, DNA, proteins and RNA [10]. In fact, the protein molecules/structures that adsorbed effortlessly on their surfaces when bound to ONCs. Over the decades, to produce the high-quality ONCs with desirable size, phase, shape and elemental compositions several strategies have been adopted including the mechanical grinding/milling, plasma induced creation and chemical routes [6,11]. Nonetheless, these growth methods are inadequate because of the poor stability of the formed ONCs, requisites of the further chemical purification, extreme-temperature reaction state, long-term consumption, and difficulty in the disruption ONCs [11,12].

In recent years, nanosecond pulse laser ablation in liquid (PLAL) strategy has been used as an adaptable and easy approach to prepare high quality customised ONCs. The PLAL method is handy owing to its simplicity, economy, and efficiency. On top, it enables the large-scale reproducibility without requiring the toxic materials. Yet again, it is versatile for fabricating the inorganic–organic NCs with unique surface chemistry and reactive quenching of the ablated species [13,14]. Using this strategy, the physical/chemical properties of the ONCs can be controlled by adjusting the pulse laser parameters (fluence/energy density, width, wavelength, repetition rate, and duration) and liquid media [13–15]. Asahi and his co-authors disclosed that the higher fluence-ablation energy leads to the smaller size of NCs depending on the laser wavelength and pulse width [15,16]. Additionally, Zhang et al reported that the continuous laser shots can increase the yield of the NCs [15]. In brief, the nature of the liquid media (solvent molecules) and ablation wavelength play an important role to deliver the promising thermodynamic conditions to obtain the NCs with required morphology (size and shape) and structure [14,16].

It has been established that the nucleation of the cinnamon nanostructures can be critically sensitive to different types of growth liquid media and laser fluence (LF), signifying their uses towards biomedical applications [9,14]. The PLAL supported growth mechanism was clarified in terms of a simple process relating to the cavitation bubble dynamic forces, plasma generation, and the impact of pulse laser factors on the formation of the ONCs [17,18]. It has been comprehended that an interrelated laser pulse with a surface cinnamon target causes the formation of expanded plasma plume and cavitation bubble. Consequently, the cavitation bubble is then collapsed, leading a spreading of Cin-NCs into the citric acid solution. In general, the cavitation bubble lifetime extends with induced by the former pulse repetition rate and increasing of LF, thus the NCs production is higher [15,18]. The mass profusion of Cin-NCs diverse to the bubble's form shows the nonappearance of high-density slope of cluster particles once the cavitation bubble has been to its maximum height. Premkumar et al. synthesised AgNPs doped cinnamon oil and evaluated their antimicrobial against E. coli and S. aureus bacteria strains [19]. The nano/micro emulsions from the cinnamon have been studied by Yildirim et al. [20] that confirmed its bioactivity against several pathogenic bacteria. The ONCs obtained from curcumin compound were indeed produced by chemical wet-milling, grinding milling and electro-hydrodynamic atomization method to test their antibacterial action [21]. Yet, growth of systematic preparation method for nature Cin-NCs with customised particle sizes and preferred antibacterial actions still remain challenging [22].

Currently, research is directed to the synthesis of high crystalline spherical nanoclusters of tailored morphology (size and shape) using the rapid, inexpensive, and contaminants free pulsed laser ablation in liquid (PLAL) technique. The impact of laser fluences on various attributes of the cinnamon nanoclusters grown inside the citric acid liquid medium was evaluated. These Cin-NCs revealed a high bioactivity when tested against two bacteria strain (Escherichia coli and Staphylococcus aureus) compared to recent studies on metals nanoparticles that are widely utilized as antibacterial agent. In addition, this study established that the pulsed laser ablation in liquid may constitute a basis for the production of Cin-NCs with desired size distribution potential for the development of nanomedicines.

2. Experimental procedures

2.1. Materials for Cin-NCs preparation

In the local supermarket, cinnamon cassia bark was procured and chopped into small pieces dimensioned of 40 mm × 10 mm × 2 mm. These small barks (utilized as a target material) were well washed in ultrasonic bath cleaner (operated duration was 30 min), then rinsed in filtered water to eliminate any impurities. Citric acid liquid form ($C_6H_8O_7$, pH ~ 4.5, Sigma-Aldrich) was utilised as medium for Cin-NCs production. Nutrient agar and Mueller-Hinton agar were collected from Merch and used as bacterial culture growth media. Besides, Penicillin-streptomycin was acquired from Sigma-Aldrich and chosen as a control for antibacterial efficacy of Cin-NCs. Alternatively, typical Gram-positive and -negative microorganism S. aureus ATCC 25923 and E. coli ATCC 11775 bacteria were congregate from the microbiology research laboratory, UTM, Malaysia.

2.2. Synthesis of Cin-NCs by PLAL method

A Nd:YAG Q-switched pulse laser of wavelength 532 nm with the controlled parameters (pulse width of 8 ns, frequency of 1 Hz, spot diameter of 2.2 ± 0.2 mm) was used to prepare the Cin-NCs. Different values of the laser fluences (LF) were 0.7 ± 0.2, 1.4 ± 0.3, 2.2 ± 0.4, 2.9 ± 0.6, 3.6 ± 0.7 and 4.3 ± 0.8 mJ/cm^2. A Pyrex vessel filled with 5 mL of the citric acid solution was utilized as the NCs growth medium. The cinnamon target was placed inside the vessel at an estimate height of 10 ± 0.1 mm from the bottom. The pulse laser at the repetition rate of 500 pulses/sec was constantly shot over the cinnamon target surface through a lens of focal length 80 mm. The exact distance between the output pulse laser and cinnamon target surface was 17 mm due to the re-compensation of the refraction of light. The vessel containing the cinnamon target was continuously rotated at the revolution of 15 rpm using a magnetic stirrer in order to keep the formed Cin-NCs well-dispersed without any aggregation.

2.3. Characterizations of Cin-NCs

Physiochemical properties such as optical absorption, morphology chemical structure and quantum yields were obtained as following. Absorption bands were determined in the wavelength range of

200–800 nm via UV–Vis analysis (PerkinElmer Lambda 25 Spectrometer with a quartz cube of path-length 1 cm). The luminescence color modification of the prepared Cin-NCs were measured using a PerkinElmer (model-LS55) PL. FTIR absorption spectra of the Cin-NCs bonds were attained on a PerkinElmer Frontier™ spectrophotometer. The BIO-TEM from Hitachi HT7700 was employed to inspect the histogram particle size distribution, shape, phase and SAED of Cin-NCs. Elemental composites of Cin-NCs were recorded using energy dispersive X-ray (EDX) analyser, wherein the EDX spectra analysis was attached (HR-TEM, Hitachi SU8020). Liquid chromatography-mass spectrometry (LC-MS) was used to evaluate the chemical composition of the prepared Cin-NCs suspended in the citric acid medium. The evaluation was performed using an Agilent Ion Mobility 6560 Q-TOF system coupled with the Agilent 1290 Infinity II UHPLC. To obtain the average diameter of Cin-NCs was carried out on dynamical light scattering (DLS, Nano-ZS90 Malvern instrument).

2.4. Antibacterial action assessment of Cin-NCs

The antibacterial effectiveness of Cin-NCs against bacterial strains was tested using the agar-well diffusion method [23]. The nutrient and Mueller-Hinton media were speared into the germ-free Petri dishes until being dried at room temperature. Afterward, the bacterial cultures from E. coli and S. aureus were swabbed orderly on agar-dishes using purified L-shape. Four holes have been made using sterilized cork borer on each Petri dishes with a diameter of 6 mm. Cin-NCs solutions of 20 µL made by varying LF (from 0.7 to 4.3 mJ/cm^2) and then dropped inside the corresponding agar. Citric acid solution (control) and normal penicillin–streptomycin (antibacterial drug) deprived of Cin-NCs solution were utilized. The occupied dishes with/without Cin-NCs were kept at a period of 24 h and 37 °C temperature. After incubation, the present of the sphere spot as called inhibition zone diameter (IZD) around the hole was studied to evaluate the antibacterial efficiency of Cin-NCs. Besides that, the optical density (OD_{600}) of bacterial growth was monitored at 600 nm by a UV–visible spectrometer (T60-PG Instrument) for each 5 h interval to 45 h. The amount of 180 µL (10^4 cells/mL) of bacteria strains (S. aureus and E. coli) were kept at a sterilise container occupied with 20 mL of Muller-Hinton medium.

3. Results and discussion

Fig. 1 elucidates the UV–visible absorption spectra of Cin-NCs before laser irradiation at 0 mJ/cm^2 and after altering LF. Flat absorption peak has been detected at 0 mJ/cm^2 without any visible solution color, indicating that the Cin molecules were not dissolved in the solution (citric acid). Up to 0.7 mJ/cm^2 of pulse laser irradiation, it visibly revealed the variation in the Cin-NCs morphology, crystallinity and size dispersion (Inset 1) [26]. Meanwhile, the enhancement in the absorption peak intensity was increased with increasing LF, suggesting that the Cin-NCs density and particle size impacted by higher LF [24]. The appearance of a weak peak followed with a blue shift (Inset 2) was consigned to the attendance of ring of benzoyl, cinnamoyl system, and aromatic amino acid groups of proteins structure in the nucleated Cin-NCs [3,4]. Where, these little absorption bands ranged of 269–266 nm were observed because of the amino acid residues in the cinnamon protein structure (tyrosine and tryptophan yielding). On top, the high absorption peaks were obtained in the range of 304–310 nm with gradual increased accompanying a blue shift (shorter wavelength) as displayed in Inset (3). This revelation was attributed to the quantum yields of Cin-NCs and the molecules interaction of citric acid solution as described elsewhere [14,24–26]. Also, it occurred due to the chemical bonds for instance the cinnamaldehyde, coumarin, eugenol, di-tetra, hexahydrocinnamon, terpenoids, caryophyllene, heterocyclic, carboxyl, ethyl cinnamate and optical absorption properties of Cin-NCs. Overall, they may be contributing to the distinctive aroma and organic activity of Cin-NCs [12]. The luminescence color modification of Cin-NCs were evaluated from the chromaticity coordinates (x,y). Fig. 1(b) illustrations the CIE 1931 chromaticity diagram of the proposed samples which were observed in the blue region.

The FTIR spectra of the as-synthesised Cin-NCs samples at varied LF in the occurrence of different functional groups (Fig. 2a). The appearance of absorption peaks of Cin-NCs revealed a minor blue shift and broad with a change in the intensities. The symmetric absorption peaks of Cin-NCs around 3392 cm^{-1} was contributed to stretching vibration hydroxyl groups (O–H) of phenols that evidently shown in Fig. 2(a, c) [3,22]. Where, the peaks symmetric/asymmetric stretching at 2097 cm^{-1} and 1648 cm^{-1} identified the presence of carbon hydroxyl (C = C groups) of aldehydes and carbony1 (C = O groups) of alkenes structure [24]. That obviously exhibited the association between the molecular structure of Cin and the solution surfactant as dot-circled in Fig. 2(b), which supported by the detected expansion and blue shift in the absorption peak of UV–Vis (Fig. 1a). This was due to the existence of the polyphenols, heterocyclic and cinnamaldehyde compounds in the Cin [9]. Furthermore, the absorption peaks were located at 1414 cm^{-1} assigned to carbon-hydroxyl groups (C-O) of aromatic amines that conjugates from aromatic ring in the Cin [25]. All these peaks confirmed the absorption of the cinnamon molecules and amide linkages of proteins attached on the surface of the NCs by different functional

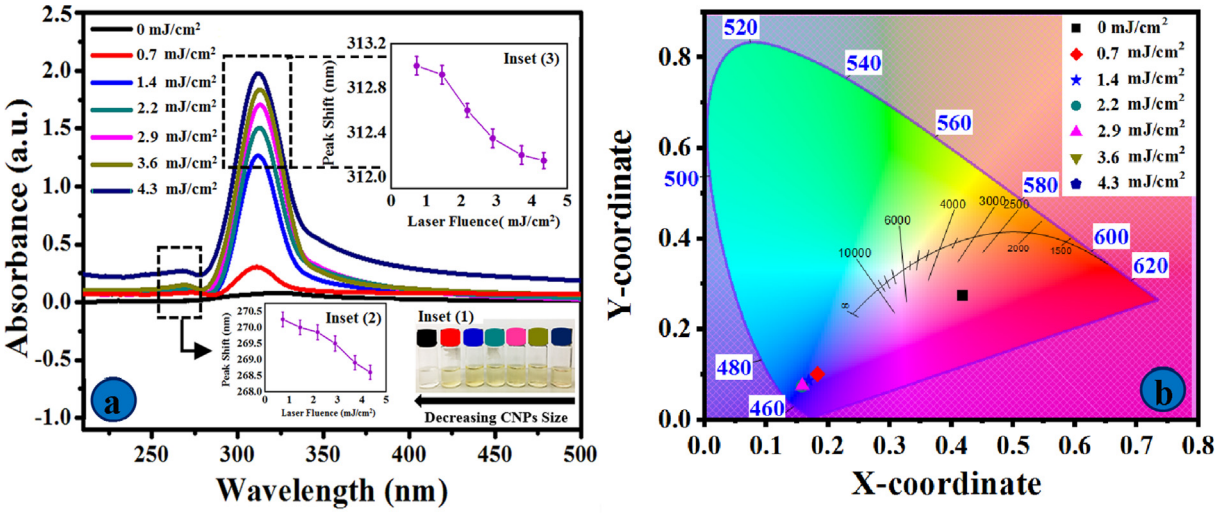

Fig. 1. (a) UV–vis spectra of the Cin-NCs prepared inside citric acid as a function of the LF. Inset (1): Cin-NCs size diameter dependent visible color change, Inset (2): absorption minor peaks shift and Inset (3): absorption prominent peaks shift, (b) the CIE 1931 chromaticity diagram.

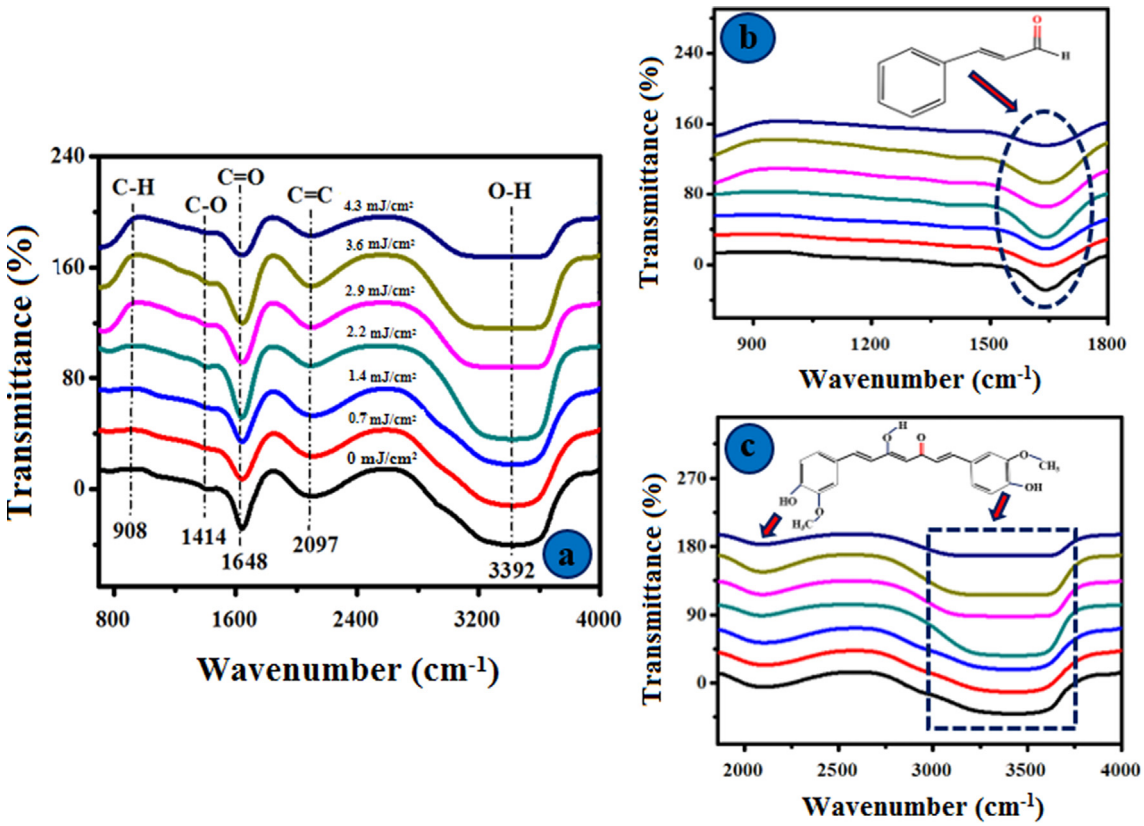

Fig. 2. FTIR absorption spectra of the Cin-NCs in the range of: (a) 750–4000 cm^{-1}, (b) 850–1800 cm^{-1}, and (c) 1700–4000 cm^{-1}.

groups as reported earlier [9,25]. The observed shift was due to the presence of the cinnamaldehyde (main compound of cinnamon) and enlargement in the particle size. Additionally, the stabilization of the Cin-NCs within the compound matrix which was attributed to the molecular interactions of the phenyls and cinnamaldehyde compounds with the surrounding citric acid molecules. Moreover, this indicated the covering of Cin-NCs by the secondary plant metabolites of (terpenoids, flavonoids, heterocyclic, aldehyde, coumarin, phenols and tannins) [22–26] which reveals new attachments to the bacterial membranes wall [14].

Fig. 3 (a-c) displays the shape, phase, particle size, elemental composite and lattice plane structure with crystalline fringe images of the finest Cin-NCs (grown at LF of 2.2 mJ/cm^2). Fig. 3 (a) showed the predominance of spherical shaped Cin-NCs grown in the solution with histogram size distribution ranged of 2–26 nm (Inset). The existence of unique spherical morphology of the Cin-NCs was ascribed to the finely created atoms that were restricted via the existing nuclei throughout the dispersion-controlled growth media that are useful for developing the antibacterial drug [23]. The EDX spectra (Fig. 3 (b)) of the obtained Cin-NCs revealed the natural elemental compositions in the presence of Si, C, O, Fe, Al, Cu, Sn and Ca. The percentage of the intense elemental peaks of C, O, Si and Al (as tabulated of the inset of Fig. 3 (b)) were ascribed to the protein capping over the Cin-NCs. The presence of various chemical compounds in the cinnamon was identified by LC/MS analysis. The LC chromatograms of the citric acid containing the cinnamon before and after the laser ablation were recorded (not shown here). The emergence of several new peaks clearly revealed the existence of the Cin-NCs in the citric acid formed by the laser ablation at optimum fluence of 2.2 mJ/cm^2.

Magnified HR-TEM images illustrated more bright edges of the particle than centers (red rectangle of selected region in the Fig. 3c), suggesting the formation of the biomolecular protein structures attached to the surface of the Cin-NCs. The profile of the lattice fringes (yellow square box, Inset c2), SAED pattern (Inset c1) and crystalline profile spacing (Inset c5) of a single Cin-NC were depicted. These observations confirmed the growth of the Cin-NCs along the preferred lattice planer direction with concentric rings and bright circular spots. Besides, the lattice spacing ($\approx$ 0.14 nm) of the NC (Inset (c3)) unveiled the consistent fringe of the lattice plane as clearly presented in the Fig. 3 c (Inset c4). Fig. 3c (Inset c6) shows the XRD patterns (in the 2θ range from 20° to 80°) of the synthesized Cin-NCs at the optimum laser fluence of 2.2 mJ/cm^2. The marked five significant diffraction peaks centered at the 2θ values of 15°, 24.4°, 30.2°, 38.2° and 52.6° were due to the growth orientation along (0 0 1), (2 2 0), (0 0 2), (3 1 1) and (4 4 0) lattice planes, respectively. These intense and sharp XRD peaks indicated the nucleation of highly crystalline face center cubic (fcc) structure of Cin-NCs (DB Card Number 01–074-9D14) wherein the width of the XRD peaks can be attributed to crystallite size of the NCs.

The DLS measurement was conducted to determine the LF dependent particle diameters of Cin-NCs together with their standard deviations. Fig. 4 (chart) clearly disclosed that the produced Cin-NCs were homogenous with smaller particle size when the LF was increased. This was due to the higher efficient passing temperature [27]. Additionally, the selected LF of 2.2 mJ/cm^2 has exposed high density and crystalline spherical Cin-NCs. The fast diffusion assisted growth of the Cin-NCs and multiphoton absorption together with the lattice oscillation was responsible for such behavior [24]. Subsequently, the fast-annealed mechanical destruction was acted before the thermal equilibrium was achieved in the citric acid solution, turning to the formation of the smaller Cin-NCs. After the diffusion of LF into the citric acid solvent, the Cin-NCs temperature was dropped to the room temperature before the following pulse laser was reached [25–29].

3.1. Antibacterial action of Cin-NCs

The S. aureus and E. coli bacterial cultures were examined on the

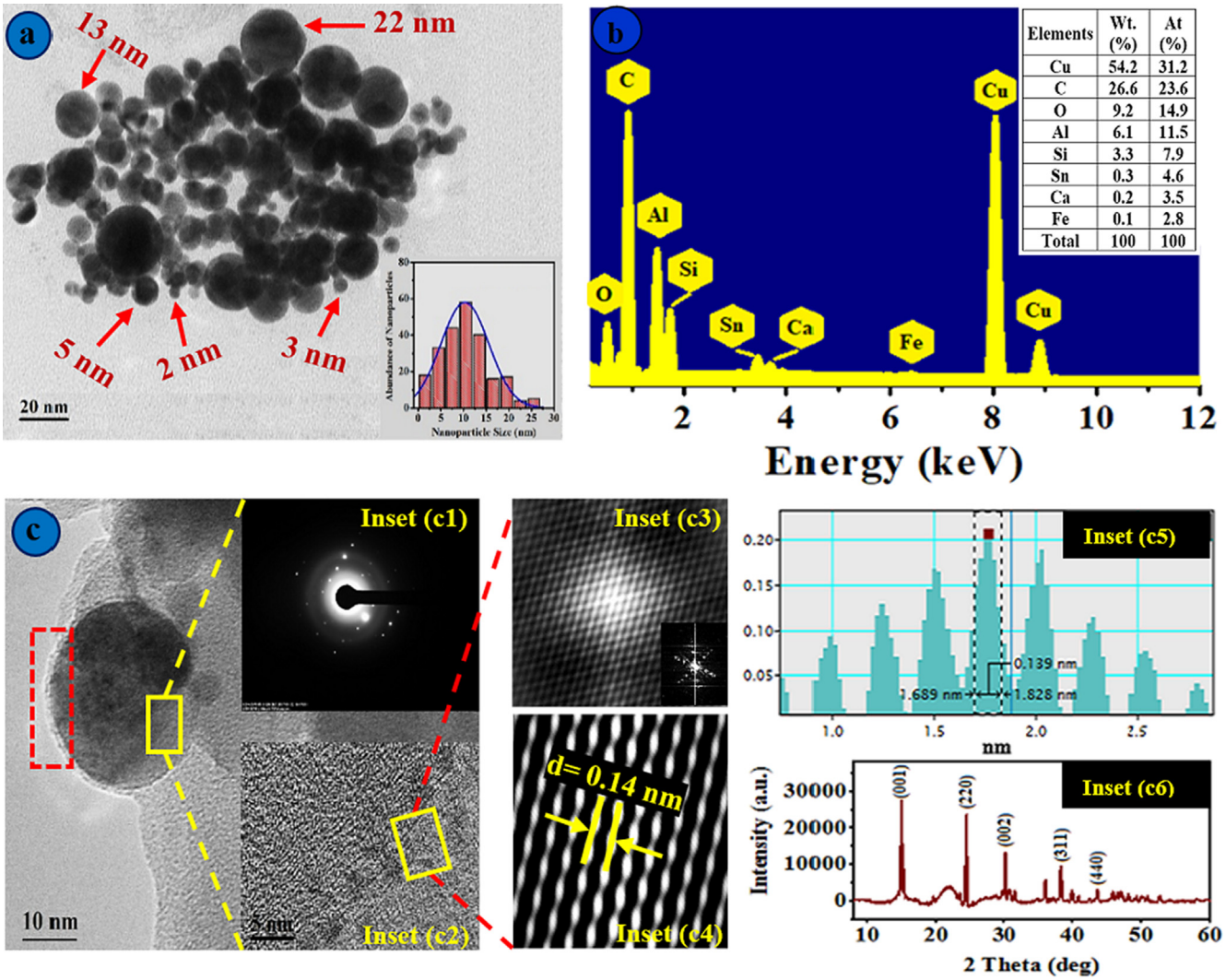

Fig. 3. The Cin-NCs produced at the LF of 2.2 mJ/cm^2: (a) HR-TEM image (top view) (Inset: histogram particle size distribution corresponding to (a) Cin-NCs), (b) EDX spectrum (Inset: Detected chemical elements At.% and Wt.%). (c) HR-TEM images (Insets: (c1) SEAD pattern, (c2), (c3) and (c4) lattice fringes, (c5) crystalline profile spacing and (c6) XRD patterns).

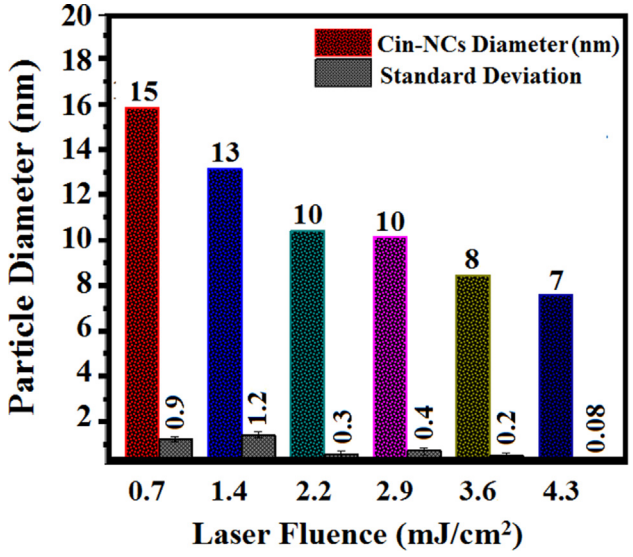

Fig. 4. The LF dependent changes in the Cin-NCs diameter (nm) with standard deviation.

agar-well diffusion process [9,23]. The IZD valuation was used to inspect the antibacterial effectiveness of the newly prepared Cin-NCs (Fig. 5 and Table 1). The Cin-NCs were filled into the holes sited on the Petri dishes as illustrated in Fig. 5A (red-circle) and the IZD surrounded the hole was measured (Fig. 5 (A,B)). All the Cin-NCs suspension and blank (citric acid solution) with varying diameters of Cin-NCs (3–26 nm) that were acquired at different LF (from 0.7 mJ/cm^2 up to 4.3 mJ/cm^2) revealed a high inhibitory impact (Fig. 5 A and B). Nevertheless, the occurrence of the broadest width of the IZD (measured in mm) that was attained for the best sample S4–90 established its highest antibacterial action.

The LF dependent particular IZD (24 and 25 mm) for the bacteria strains *E. coli* and *S. aureus* were matched with the selected antibiotic agent (Fig. 5 (A,a) and (B,b)). The detected assortment in the antibacterial drug (Cin-NCs) was due to the alterations in the bacterial cell wall membrane structure [2], wherein this cell wall of E. coli bacteria was encompassed to the actual thin lipopolysaccharide and a peptidoglycan [30]. These lipopolysaccharides and polysaccharides structures were both comprised of the coupled lipids with negative charges, indicating that a less permeability into the Cin-NCs. Contrariwise, the bacteria membrane structure of *S. aureus* created a thick peptidoglycan, enfolding of linear polysaccharide chains cross connected by small peptides to construct a static structure in 3-D that trapped the

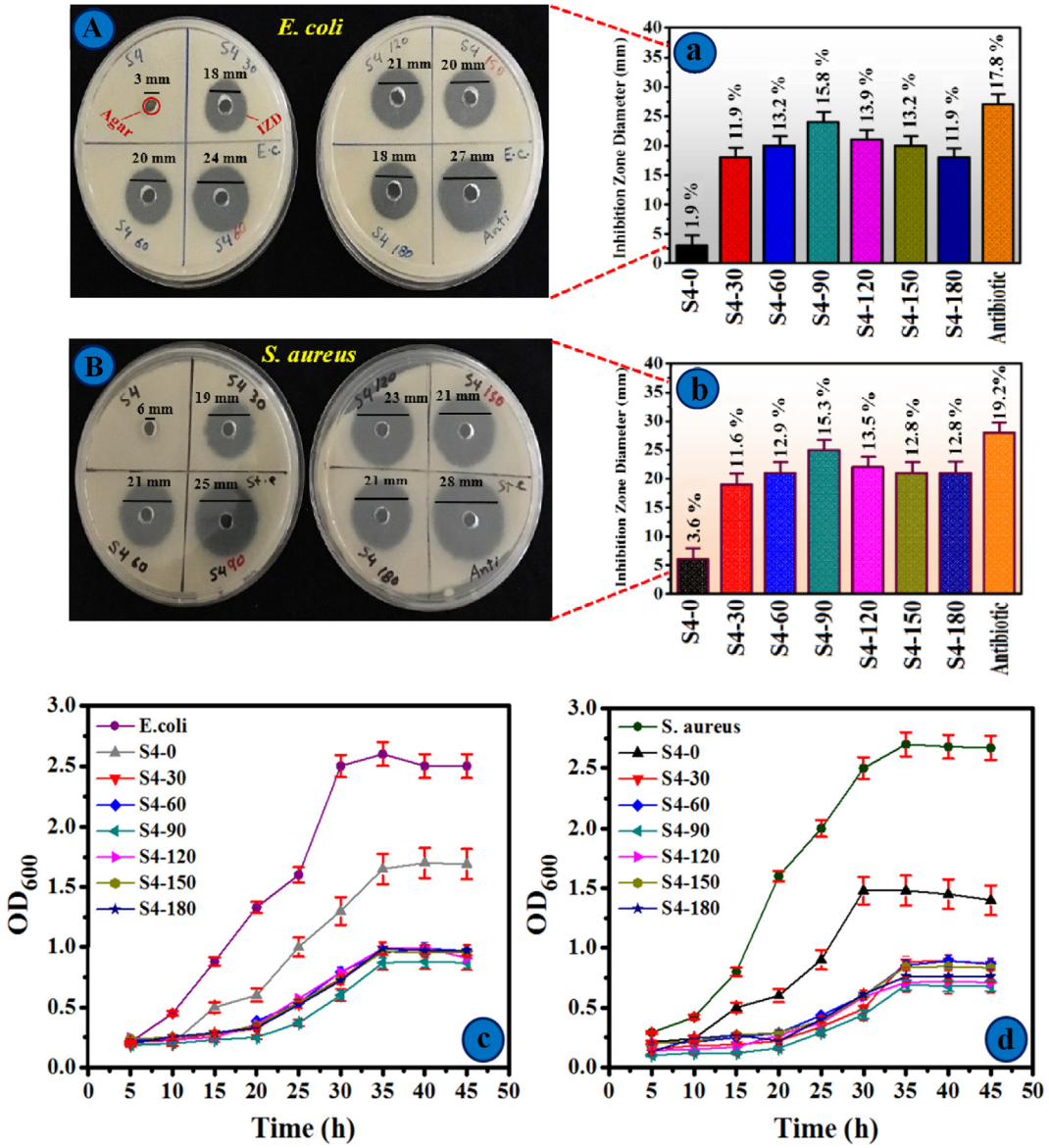

Fig. 5. The antibacterial action showing the (A,B) inhibition zone diameter and (c,d) growth profile of the Cin-NCs in the citric acid medium (at 37 °C) synthesised at different LF against *E. coli* and *S. aureus* bacteria, (a,b) the inhibition activity of the Cin-NCs.

Table 1
The LF/PLAE dependent Cin-NCs diameter (± standard deviation, SD) and sample code (NA: not applicable).

Cin-NCs sample code	LF (mJ/cm^2)	Diameter ± SD (nm)	IZD of E. coli (mm)	IZD of S. aureus (mm)
S4-0	0	NA	3	6
S4-30	0.7	15 ± 0.9	18	19
S4-60	1.4	13 ± 1.2	20	21
S4-90	2.2	10 ± 0.3	24	25
S4-120	2.9	10 ± 0.4	21	23
S4-150	3.6	8 ± 0.2	20	21
S4-180	4.3	7 ± 0.08	18	21
Antibiotic	NA	NA	27	28

permeation of the Cin-NCs to the bacteria structure [30]. The obtained IZD for the Cin-NCs revealed to be higher than the earlier reported values [9,31–35]. This outcome was attributed to the existence of cinnamaldehyde, flavonoids, cinnamic, polyphenols, heterocyclic and the coumarin constituents [6,11].

Several mechanisms have been proposed for the ONCs as antibacterial agent [30–32]. According to Feng et al. [31], the mechanism and association revisions of the antibacterial effectiveness to the separation of cytoplasm membrane cell can verify the destruction of the duplicate ability of DNA and the protein annihilation in the bacteria. Furthermore, Shrivastava et al. [32] inspected the interface of the *E. coli* and *S. aureus* bacterial cell wall with interrelated Cin-NCs where the altering tyrosine phosphorylation structures were agued to be the reason for the antibacterial efficiency of the nanostructures.

The mechanism behind the antibacterial potency of the proposed Cin-NCs is related to their unique physiochemical attributes that enable the penetration through the cell membrane to create oxidative stress. Consequently, the protein sortase at the bacterial cell surface are efficiently inhibited, preventing the coalescence of the bacterial cells to fibronectin. The results affirmed that the Cin-NCs can adhere onto the bacterial cell walls and break them before being infiltrated within the membrane to rupture chemical components of the cell organelles. It has been established that the tinier nanoparticles reveal stronger bactericidal properties. Lee et al. [33] reported that nanoparticles with mean size range from 5 to 80 nm can destroy the microorganisms (bacteria such as the *S. aureus* and *E. coli*) by penetrating inside the bacterial cell

Table 2
Comparative evaluation of Cin-NCs prepared at different liquid media at optimum growth condition.

Properties of cinnamon nanoparticles	Methanol liquid	Ethanol liquid	Citric acid liquid
Morphology	Elliptical	Spherical	Spherical
Density (g/cm3)	0.821	0.835	1.713
Mean Size (nm)	28	9	10
Lattice Spacing (nm)	0.216	0.241	0.14
Absorbance (nm)	261 and 321	260 and 320	269 and 310
Antibacterial Test (IZD in mm)	20–22	20–23	19–25

membranes. In fact, tinier Cin-NCs can rupture efficiently the intracellular oxygen bonds, resulting in the severe oxidative damages and thus allowing the ultimate destruction of the bacterial cells membrane.

Fig. 5(c) and (d) illustrates the growth of the *E. coli* and *S. aureus* in the LB media, detected under the optical density (OD_{600}) with different LF. The antibacterial activity of the Cin-NCs (particle diameter) were examined on the blank suspension (citric acid) and containing Cin-NCs (synthesis at varied LF) for each 5 h interval duration up to 45 h. Our results for optimum sample S4-90 showed that the lower OD_{600} of bacteria containing Cin-NCs after cultivation for a proper time verified the strongest antibacterial activity (Fig. 5 (c, d)) and Table 1). This disclosure was accredited to the influence of the Cin-NCs on the intracellular materials and subsequent destruction of the bacterial membrane structure that caused the coagulation and removal of cells in the liquid system. In addition, the Cin-NCs (S4-90 sample) with mean size of 10 ± 0.3 nm had appreciable effect against the bacterial growth. This was due to the large surface area to volume ratio of the Cin-NCs that has strong interfacial interaction with the bacterial membranes structure [34,35].

3.2. Comparative evaluation of Cin-NCs

The morphological analysis of the Cin-NCs having controlled properties produced inside different growth media including ethanol and methanol using the PLAL technique with varied laser parameters was reported [9,35]. However, the structural and antibacterial traits of the Cin-NCs produced in the citric acid media have never been evaluated. Thus, the main purpose of this paper is to determine the feasibility of achieving some better Cin-NCs morphologies and structures

inside the citric acid as the growth media with enhanced antibacterial efficiency. Unique traits of these Cin-NCs were well analysed and determined using different spectroscopic and imaging tools. The morphology (size, shape and structure) and optical characteristics of these Cin-NCs were found to be sensitive to the nature of the liquid media and laser fluences. The antibacterial effectiveness of these Cin-NCs was evaluated against different bacteria strains. All the liquid media were favorable for synthesizing the Cin-NCs with strong antibacterial activity. In the present work, these spherical Cin-NCs with high chemical stability produced inside the citric acid medium (pH 4.5) demonstrated to have strongest antibacterial effectiveness, Especially, the presence of these Cin-NCs surrounded by the citric acid molecules have great physical properties compared to other media (ethanol and methanol) as shown in Table 2. These observations can be attributed to the high crystallinity of the Cin-NCs achieved via the optimized PLAL technique. Besides, these Cin-NCs grown inside the citric acid media showed excellent spherical morphologies, indicating their higher potential to delay the bacterial growth more efficiently than those produced inside methanol and ethanol. It is established that the PLAL technique may constitute a basis for the production of the Cin-NCs with desired characteristics useful for the development nanomedicines towards the protein spikes of coronavirus and antibacterial drug design.

4. Conclusions

The natural Cin-NCs were synthesised for the first time using as accurate and high purity PLAL (at fundament wavelength of 532 nm) technique. As-prepared NCs were characterised to analyses their structural, optical and antibacterial properties. These Cin-NCs were produced inside the liquid citric acid medium (acted as organic solvent) at various LF in a customized way. The influence of various LF on the structure, morphology, optical and bactericidal properties of the Cin-NCs were determined. The citric acid as a growth medium was demonstrated to be more promising for the fabrication of tiny spherical crystalline Cin-NCs with uniform distribution. In addition, the proposed PLAL method exhibited high productivity of NPs in the absence of any toxic chemicals that is demanding for the future antibacterial drug development. The strong UV–Vis optical absorption at 269 and 310 nm shown by the Cin-NCs may be beneficial for new drug formulation. The FTIR spectra of the Cin-NCs confirmed the existence of the symmetric-asymmetric stretching vibrations bands of the active component (polyphenols and cinnamaldehyde functional groups with characteristic bonds). The selected LF of 2.2 mJ/cm^2 produced the best Cin-NCs (size and shape) with the mean diameter of approximately 10 ± 0.3 nm. The antibacterial effectiveness of the Cin-NCs were evaluated against *Escherichia coli* and *Staphylococcus aureus* bacterial cultures through the IZD and OD_{600} analyses. The best Cin-NCs (S4-90) revealed the strongest antibacterial action (IZD of 24 mm for *S.aureus* and 25 mm for *E. coli*). This outstanding antibacterial activity shown by the Cin-NCs was due to their high quantum yield, high stability and well-defined morphology. Also, the OD_{600} of the Cin-NCs affirmed their exceptional antibacterial potency when implemented on the bacterias growth over the time intervals of 5 up to the total of 45 h. In short, the PLAL supported growth process/mechanism and the antibacterial efficacy of the produced Cin-NCs was well-understood. The proposed Cin-NCs may be potential for the antibacterial drug formulation.

Declaration of Competing Interest

The authors declare that they have no known competing financial interests or personal relationships that could have appeared to influence the work reported in this paper.

Acknowledgments

The authors appreciate the financial support from RMC-UTM 04E86, MOHE FRGS 5F050 UTMFR 20H65.

References

[1] E.D. Brown, G.D. Wright, Antibacterial drug discovery in the resistance era, Nature 529 (2016) 336–343.
[2] D.M. Morens, G.K. Folkers, A.S. Fauci, The challenge of emerging and re-emerging infectious diseases, Nature 430 (2004) 242.
[3] Y. Zhang, X. Liu, Y. Wang, P. Jiang, S. Quek, Antibacterial activity and mechanism of cinnamon essential oil against Escherichia coli and Staphylococcus aureus, Food Control 59 (2016) 282–289.
[4] M. Sathishkumar, K. Sneha, S.W. Won, C.W. Cho, S. Kim, Y.S. Yun, Cinnamon zeylanicum bark extract and powder mediated green synthesis of nano-crystalline silver particles and its bactericidal activity, Colloids Surf., B 73 (2009) 332–338.
[5] B. Shan, Y.Z. Cai, J.D. Brooks, H. Corke, Antibacterial properties and major bioactive components of cinnamon stick (cinnamomum burmannii): activity against foodborne pathogenic bacteria, J. Agric. Food. Chem. 55 (2007) 5484–5490.
[6] Y.H. Wang, B. Avula, N.D. Nanayakkara, J. Zhao, I.A. Khan, Cassia cinnamon as a source of coumarin in cinnamon-flavored food and food supplements in the United States, J. Agric. Food. Chem. 61 (2013) 4470–4476.
[7] R. Thada, S. Chockalingam, R.K. Dhandapani, R. Panchamoorthy, Extraction and quantitation of coumarin from cinnamon and its effect on enzymatic browning in fresh apple juice: a bioinformatics approach to illuminate its anti-browning activity, J. Agric. Food. Chem. 61 (2013) 5385–5390.
[8] D. Gunawardena, N. Karunaweera, S. Lee, F. van Der Kooy, D.G. Harman, R. Raju, G. Münch, Anti-inflammatory activity of cinnamon (C. zeylanicum and C. cassia) extracts identification of E-cinnamaldehyde and o-methoxy cinnamaldehyde as the most potent bioactive compounds, Food Function 6 (2015) 910–919.

[9] A.A. Salim, N. Bidin, A.S. Lafi, F.Z. Huyop, Antibacterial activity of PLAL synthesized nanocinnamon, Mater. Des. 132 (2017) 486–495.
[10] M. Xie, D. Fan, Z. Zhao, Z. Li, G. Li, Y. Chen, M. Zhi, Nano-curcumin prepared via supercritical: Improved anti-bacterial, anti-oxidant and anti-cancer efficacy, Int. J. Pharm. 496 (2015) 732–740.
[11] J.P. Sylvestre, M.C. Tang, A. Furtos, G. Leclair, M. Meunier, J.C. Leroux, Nanonization of megestrol acetate by laser fragmentation in aqueous milieu, J. Control. Release 149 (2011) 273–280.
[12] S. Zhang, M. Zhang, Z. Fang, Y. Liu, Preparation and characterization of blended cloves/cinnamon essential oil nanoemulsions, LWT-Food Sci. Technol. 75 (2017) 316–322.
[13] T. Tsuji, K. Iryo, Y. Nishimura, M. Tsuji, Preparation of metal colloids by a laser ablation technique in solution: influence of laser wavelength on the ablation efficiency, J. Photochem. Photobiol. A: Chem. 145 (2001) 201–207.
[14] A.A. Salim, N. Bidin, Pulse Q-switched Nd: YAG laser ablation grown cinnamon nanomorphologies: Influence of different liquid medium, J. Mol. Struct. 11 (2017) 694–700.
[15] D. Zhang, B. Gökce, S. Barcikowski, Laser synthesis and processing of colloids: fundamentals and applications, Chem. Rev. 117 (2017) 3990–4103.
[16] T. Asahi, T. Sugiyama, H. Masuhara, Laser fabrication and spectroscopy of organic nanoparticles, Acc. Chem. Res. 41 (2008) 1790–1798.
[17] P. Wagener, A. Schwenke, B.N. Chichkov, S. Barcikowski, Pulsed laser ablation of zinc in tetrahydrofuran: bypassing the cavitation bubble, J. Phys. Chem. C 114 (2010) 7618–7625.
[18] R. Streubel, S. Barcikowski, B. Gökce, Continuous multigram nanoparticle synthesis by high-power, high-repetition-rate ultrafast laser ablation in liquids, Opt. Lett. 41 (2016) 1486–1489.
[19] J. Premkumar, T. Sudhakar, A. Dhakal, J.B. Shrestha, S. Krishnakumar, P. Balashanmugam, Synthesis of silver nanoparticles (AgNPs) from cinnamon against bacterial pathogens, Biocatal. Agricultural Biotechnol. 15 (2018) 311–316.
[20] S.T. Yildirim, M.H. Oztop, Y. Soyer, Cinnamon oil nanoemulsions by spontaneous emulsification: Formulation, characterization and antimicrobial activity, LWT-Food Sci. Technol. 84 (2017) 122–128.
[21] R.K. Basniwal, H.S. Buttar, V.K. Jain, N. Jain, Curcumin nanoparticles: preparation, characterization and antimicrobial study, J. Agric. Food. Chem. 59 (2011) 2056–2061.
[22] X. Zeng, X. Mao, S.S. Mao, S.B. Wen, R. Greif, R.E. Russo, Laser-induced shockwave propagation from ablation in a cavity, Appl. Phys. Lett. 88 (2006) 061502.
[23] R.C. Goy, S.T. Morais, O.B. Assis, Evaluation of the antimicrobial activity of chitosan and its quaternized derivative on E. coli and S. aureus growth, Revista Brasileira de Farmacognosia 26 (2016) 122–127.
[24] T. Tanaka, Y. Matsuo, Y. Yamada, I. Kouno, Structure of polymeric polyphenols of cinnamon bark deduced from condensation products of cinnamaldehyde with catechin and procyanidins, J. Agric. Food. Chem. 56 (2008) 5864–5870.
[25] N. Jeyaratnam, A.H. Nour, R. Kanthasamy, A.H. Nour, A.R. Yuvaraj, J.O. Akindoyo, Essential oil from cinnamomum cassia bark through hydro distillation and advanced microwave assisted hydro distillation, Ind. Crops Prod. 92 (2016) 57–66.
[26] L.B. Gende, I.R. Floris, M.J. Fritz, Antimicrobial activity of cinnamon (cinnamomum zeylanicum) essential oil and its main components against Paenibacillus larvae from *Argentine*, Bull. Insectology 61 (2008) 1.
[27] T. Asahi, K. Yuyama, T. Sugiyama, H. Masuhara, Preparation of organic dye nanoparticles by nanosecond laser ablation in a poor solvent, Rev. Laser Eng. 33 (2005) 4–46.
[28] B. Li, T. Kawakami, M. Hiramatsu, Enhancement of organic nanoparticle preparation by laser ablation in aqueous solution using surfactants, Appl. Surf. Sci. 210 (2003) 171–176.
[29] S.I. Kudryashov, A.A. Samokhvalov, A.A. Nastulyavichus, I.N. Saraeva, V.Y. Mikhailovskii, A.A. Ionin, V.P. Veiko, Nanosecond-laser generation of nanoparticles in liquids: From ablation through bubble dynamics to nanoparticle yield, Materials 12 (2019) 562.
[30] D.P. Tamboli, D.S. Lee, Mechanistic antimicrobial approach of extracellularly synthesized silver nanoparticles against gram positive and gram-negative bacteria, J. Hazard. Mater. 260 (2013) 878–884.
[31] Q.L. Feng, J. Wu, G.Q. Chen, F.Z. Cui, T.N. Kim, J.O. Kim, A mechanistic study of the antibacterial effect of silver ions on Escherichia coli and Staphylococcus aureus, J. Biomed. Mater. Res. 52 (2000) 662–668.
[32] S. Shrivastava, T. Bera, A. Roy, G. Singh, P. Ramachandrarao, D. Dash, Characterization of enhanced antibacterial effects of novel silver nanoparticles, Nanotechnology 18 (2007) 225-103.
[33] C. Lee, J.Y. Kim, W.I. Lee, K.L. Nelson, J. Yoon, D.L. Sedlak, Bactericidal effect of zero valent iron nanoparticles on Escherichia coli, Environ. Sci. Technol. 42 (2008) 4927–4933.
[34] I. Sondi, B. Salopek-Sondi, Silver nanoparticles as antimicrobial agent: a case study on E. coli as a model for Gram-negative bacteria, J. Colloid Interface Sci. 275 (2004) 177–182.
[35] A.A. Salim, N. Bidin, S.K. Ghoshal, Growth and characterization of spherical cinnamon nanoparticles: Evaluation of antibacterial efficacy, LWT 90 (2018) 346–353.